Mining moon & mars with microbes

Biological approaches to extract iron from Lunar and Martian regolith

Volger, R.; Pettersson, G.M.; Brouns, S. J.J.; Rothschild, L. J.; Cowley, A.; Lehner, B. A.E.

DOI
10.1016/j.pss.2020.104850

Publication date
2020

Document Version
Accepted author manuscript

Published in
Planetary and Space Science

Mining Moon & Mars with microbes: Biological approaches to extract iron from Lunar and Martian regolith

Authors: **R. Volger[a], G. M. Pettersson[b], S.J.J. Brouns[c], L.J. Rothschild[d], A. Cowley[e]* and B. A. E. Lehner[f]***

Abstract

The logistical supply of terrestrial materials to space is costly and puts limitations on exploration mission scenarios. *In-situ* resource utilization (ISRU) can alleviate logistical requirements and thus enables sustainable exploration of space. In this paper, a novel approach to ISRU, utilizing microorganisms to extract iron from Lunar or Martian regolith, is presented. Process yields, and kinetics are used to verify the theoretical feasibility of applying four different microorganisms. Based on yields alone, three of the four organisms were not investigated further for use in biological ISRU. For the remaining organism, *Shewanella oneidensis*, the survivability impact of Martian regolith simulant JSC-MARS1 and Mars-abundant magnesium perchlorate were studied and found to be minimal. The payback time of the infrastructure installation needed for the process with *S. oneidensis* on Mars was analyzed and the sensitivity to various parameters was investigated. Water recycling efficiency and initial regolith concentration were found to be key to process performance. With a water recycling efficiency of 99.99% and initial regolith concentration of 300 g/L, leading to an iron concentration of approximately 44.7 g/L, a payback time of 3.3 years was found.

1. Introduction

The next step in human space exploration will revolve around the Moon, as a stepping stone for an eventual human presence on Mars (NASA, 2018). In the context of longer stays on the Moon's surface, the supply and maintenance of a functional habitat requires the input of resources. Transport of these resources is a major cost for an extraterrestrial base, and reducing this cost will bring us closer to realizing a sustained human presence on another celestial body (Carpenter et al., 2016). *In situ* resource utilization (ISRU), the use of local resources for production and maintenance, can help us bring down long-term transport requirements and brings us closer to colonizing another celestial body (Culbert et al., 2015). In this paper, we help to address this challenge by investigating the use of microorganisms for the extraction of metals from Lunar and Martian regolith.

Microorganisms as used in production processes can be described as self-reproducing modifiable nano-factories, catalyzing a wide range of chemical conversions. Some branches of microbial life on earth have developed a metabolism around the use of metal oxides as electron donors or acceptors (Weber et al., 2006). A subsection of these organisms can utilize solid metal oxides as substrate, converting them to more soluble forms,

which makes them interesting for use in mining operations (Valdés et al., 2008). Such use of microorganisms on earth is widespread and is actively used in the biomining of copper, cobalt, gold, uranium and other metals (Rawlings, 2002; Schippers et al., 2013). In the case of copper, biomining accounts for more than 20% of the yearly worldwide production (Yin et al., 2018). These facts give a promising outlook on the application of biomining in space exploration (Cousins and Cockell, 2016). Lab-scale experiments on the interaction between bacteria and lunar regolith simulant confirm this expectation (Navarrete et al., 2013). However, so far, no design for full-scale biomining operations in space has been presented.

Iron is one of the most utilized metals on Earth, most of our building materials rely on it in some way. It can be hypothesized that the construction and maintenance of an extraterrestrial base will also rely on iron. Considering the abundance of iron in both Lunar and Martian regolith, at 5-22 wt% and 17.9 $\pm$0.6 wt%, respectively (Halliday et al., 2001; Lawrence et al., 2002), this element is likely to be useful in construction-oriented ISRU.

With this work, we show a general setup for a biological iron extraction process, we investigate the feasibility of several candidate organisms and perform a sensitivity analysis for the biological process. Combined with a lander concept (Lehner et al., 2019) , this provides a framework for future evaluations of biomining processes in space exploration and a basis for evaluation of other bioprocesses.

2. Materials & Methods

2.1. Kinetic models

Growth kinetics for *Escherichia coli*, *Magnetospirillum gryphiswaldense*, *Shewanella oneidensis* MR-1 and *Acidithiobacillus ferrooxidans* were derived from literature (Table 1 & SI) and combined with mass balances for the relevant chemical compounds. The resulting system of differential equations was solved with the MATLAB ode15s or ode45 solver. Similar initial concentrations were chosen for all simulations (Table 2). Growth on lactate was considered for all heterotroph organisms (*S. oneidensis, M. Gryphiswaldense, E. coli)*. Only *A. ferrooxidans* uses CO_2 as a carbon source and grows autotrophically. Production of acetate by both *S. oneidensis* and *E. coli* is indicated in table 1, but inhibitory effects are not considered in their models.

A. ferrooxidans grows aerobically and shows oxygen-limited behavior at concentrations below 1 mg / L ($3.1*10^{-2}$ mM) (Liu et al., 1988). The current kinetics hold if the concentration remains above this level. The inhibition by Fe^{3+} is considered in the model.

Table 1. Kinetic characteristics and expected byproducts for each proposed organism. Both *E. coli* and *M. gryphiswaldense* are intended for accumulation of dissolved iron in magnetic forms, while *A. ferrooxidans* and *S. oneidensis* are utilized for the extraction of iron from minerals.

Organism	**Byproducts**	**Kinetics**	**Parameters**
E. coli (Hua et al., 2007; Núñez et al., 2002)	Acetate	$\mu = \mu_{max} * \frac{c_{Lac}}{c_{Lac} + K_{Lac}} * \frac{c_{O2}}{c_{O2} + K_{O2}}$	$\mu_{max} = 0.22\ h^{-1}$ $K_{Lac} = 10\ \mu M$ $K_{O2} = 0.01\ mM$
M. gryphiswaldense (Naresh et al., 2012)		$\mu = \mu_{max} * \min(f_{NO_3}, f_{Lac})$ $f_{NO_3} = 0.5 + 0.5 * \frac{c_{NO_3}}{c_{NO_3} + K_{NO_3}}$ $f_{Lac} = \frac{c_{Lac}}{c_{Lac} + K_{Lac}}$	$\mu_{max} = 0.15\ h^{-1}$ $K_{Lac} = 1\ mM$ $K_{NO_3} = 0.2\ mM$
S. oneidensis (Feng et al., 2012; Kostka et al., 2002, 1996; Liu et al., 2002; Pinchuk et al., 2010)	Acetate	$\mu = \mu_{max} * \frac{c_{Lac}}{c_{Lac} + K_{Lac}} * \frac{c_{Fe^{3+}}}{c_{Fe^{3+}} + K_{Fe^{3+}}}$	$\mu_{max} = 0.1\ h^{-1}$ $K_{Lac} = 19.4\ mM$ $K_{Fe^{3+}} = 0.55\ mM$
A. ferrooxidans (Liu et al., 1988; Molchanov et al., 2007; Navarrete et al., 2013)		$\mu = \mu_{max} * \frac{c_{Fe^{2+}}}{c_{Fe^{2+}} + K_{Fe^{2+}}} * \frac{K_{Fe^{3+}}}{c_{Fe^{3+}} + K_{Fe^{3+}}}$	$\mu_{max} = 0.082\ h^{-1}$ $K_{Fe^{2+}} = 0.072\ mM$ $K_{Fe^{3+}} = 2.5\ mM$

Table 2. Initial conditions used for solving the kinetic models of the different organisms. Concentrations in mol / L, biomass concentration in Cmol / L.

	Lactate	Fe^{2+}	Fe^{3+}	NH_4^+	O_2	CO_2	Biomass
E. coli	0.08	0.15	0	0.02	$2.5*10^{-4}$	0	$4.0*10^{-4}$
M. gryphiswaldense	0.08	0.15	0	0.035	$2.5*10^{-4}$	0	$4.9*10^{-4}$
S. oneidensis	0.08	0	0.15	0.001	$2.5*10^{-4}$	0	$4.8*10^{-4}$

A. ferrooxidans	0	0.15	0.005	0.001	$2.0*10^{-4}$	$1.5*10^{-4}$	$3.7*10^{-4}$

The biomass mass balance was set up as follows:

$$\frac{dc_X}{dt} = \mu * c_X \quad (1)$$

And for the relevant chemical species in i:

$$\frac{dc_i}{dt} = Y_{i/_X} * \mu * c_X \quad (2)$$

In the case of gaseous components, a mass transfer term was included:

$$\frac{dc_i}{dt} = Y_{i/_X} * \mu * c_X + (k_L a)_i * \left(c^*_{l,i} - c_{l,i}\right) \quad (3)$$

The internal pressure is assumed to be 1 bar. When the process requires O_2 and CO_2, a gas composition with 21% O_2, 0.05% CO_2 and an inert gas such as N_2 for the remainder is assumed. In the anaerobic processes, the medium will be continuously sparged with an inert gas to induce mixing. The composition could be further tuned if an otherwise feasible process is slowed down significantly due to the gas-liquid mass transfer (Doran, 2013).

The maximum concentration dissolved gas ($c^*_{l,i}$) was determined by Henry's law. The values for $k_L a$, which combines interfacial area and diffusivity, were assumed to be 10.8 and 8.6 h^{-1} for O_2 and CO_2, respectively. The value for CO_2 is slightly lower because of the larger molecule size, which slows diffusion. These values are chosen on the low end of typical $k_L a$ values for slurry bioprocesses on earth (Neale and Pinches, 1994; Schumpe et al., 1987; Van Weert et al., 1995; Zokaei-Kadijani et al., 2013) to account for the decreased volumetric gas-liquid mass transfer in a reduced gravity setting (Pettit and Allen, 1992).

The process stoichiometry for the *S. oneidensis* process, which was found to be the only feasible process under our current conditions, is presented in equation 4. In Table 3 this stoichiometry is combined with the precipitation of magnetite, counteracting the acid requirements of the *S. oneidensis* reaction.

$$\begin{aligned} &18.13\ C_3H_5O_3^- + 35.34\ Fe_2O_3 + 0.154\ NH_4^+ + 141.48H^+ \\ &\rightarrow 17.8\ C_2H_3O_2^- + 17.8\ CO_2 + 70.67\ Fe^{2+} + 1\ CH_{1.66}O_{0.27}N_{0.2} + 88.94\ H_2O \end{aligned} \quad (4)$$

2.2. Shewanella growth

Shewanella oneidensis MR-1 (ATCC® 700550™) and *Shewanella oneidensis* ANA-3 (Wang et al., 2011) were aerobically cultured in Tryptic Soy Broth (TSB) media overnight at 30°C under continuous shaking (250 rpm). Different concentrations and compositions of JSC-MARS1 (0.5 g/L or 5 g/L) and Mg(ClO4)2 (0.06 M

or 6 M) were added. Thereafter, the growth behavior was observed for 48 hours by optical density (O.D.) measurements at a wavelength of 650 nm using a 96-well plate in a plate reader.

2.3. Payback time analysis

For analysis of the payback time, the approach to the kinetics and mass balances was repeated. The mass of the lander was approximated by first estimating the mass of the basic components (Volger et al., 2018). The mass of the 1 m^3 cylindrical reactor was assumed to be 250 kg, filled with 700 L of water. Measuring devices and peripherals were assumed to add 100 kg. The equipment for water recovery was estimated to weigh 100 kg. The rover collecting regolith was assumed to weigh 300 kg. Power supply is covered with an RTG of 500 kg, which covers peak power consumption of the bioprocess, and can be used to power other processes at a Martian colony when the bioprocess needs less power. The resulting mass of the basic components (1950 kg) was combined with the variable mass of water and nutrients and multiplied by 3 to account for structural components and a maturity margin. To get to an estimated launch price, SpaceX's listed price for the launch of up to 8.000 kg to GTO with a reusable rocket (SpaceX, 2019) was multiplied by a factor five to get an estimate for a launch to Mars at maximum capacity, resulting in a price of about $25.000 per kg. The SLS rocket aims at a cost of about $15.000 per kg transported to Mars (Dumbacher, 2014; Potter et al., 2018). With these estimations in mind, a launching cost of $ 20.000 per kg was assumed, which would correspond to a total cost of $ 117 million. The mass of nutrients and water was minimized to obtain the minimal payback time. With this approach, the nutrient supply runs out when the extracted iron mass equals the total initial lander mass (including nutrients). Increased nutrient and water supplies result in a slightly longer payback time, but a final iron production exceeding the initial lander mass.

The system provides its own power through the addition of an RTG, which is sized for use during the evaporation phase of the process and thus has an overcapacity during the other process phases. In terms of maintenance, the system is intended to be an autonomous reactor system requiring no astronaut intervention.

3. Results & Discussion

3.1. Biomining process

The general process of using bacteria for mining applications in space, is the dissolution and accumulation of specific resources from Lunar or Martian regolith (Fig 1A). The biological methodologies can be split up in two categories (Fig 1B, 1C):

1. Accumulation of dissolved iron in concentrated form, allowing for magnetic extraction.

2. Leaching of iron from mineral ores, bringing it in a dissolved state, allowing for precipitation of magnetic particles and ores.

These categories could be combined to allow for the magnetic extraction of iron from a variety of ferrous mineral ores. The leaching process alone can also be combined with electrochemical manipulation of the solution to promote magnetite precipitation (Bale et al., 2016; Lozano et al., 2017; R. Dasgupta and L. Mackay, 1959).

The considered candidates for the accumulation are a genetically modified *Escherichia coli* strain and the magnetotactic wildtype bacterium *Magnetospirillum gryphiswaldense*. The constructed *E. coli* overexpresses a modified ferritin complex, has a dysfunctional iron export mechanism and an improved iron import mechanism (He et al., 2016). The combination of those modifications leads to a high intracellular iron concentration.
M. gryphiswaldense accumulates iron to produce magnetosomes, intracellular vesicles filled with magnetite that form a backbone for the organism (Lefèvre et al., 2011). The resulting capability to swim along magnetic field lines is commonly known as magnetotactic behavior (Schüler and Baeuerlein, 1998). *M. gryphiswaldense* readily uses lactate as electron donor and carbon source.

For the bioleaching category, *Shewanella oneidensis* and *Acidithiobacillus ferrooxidans* were considered. *S. oneidensis* is well-known for its capability to use a wide range of electron acceptors (Myers and Nealson, 1988), one of which is Fe^{3+}, both in aqueous and solid state (Kostka et al., 2002, 1996). Fe^{3+} from mineral sources is converted into Fe^{2+}, which is both excreted in aqueous form and precipitated on the cell surface in magnetite (Bennett et al., 2015; Perez-Gonzalez et al., 2010). In the current work, the use of lactate as electron donor and carbon source is considered, which is then oxidized to acetate and CO_2 (Fig 1C). Other possible electron donors are pyruvate, formate, amino acids or N-acetylglucosamine (Kane et al., 2016; Lovley et al., 1989).

A. ferrooxidans is often used in biomining operations on earth (Valdés et al., 2008). It preferably grows in very acidic conditions (pH 1-2) and can fix both carbon and nitrogen from atmospheric sources. For the current work, nitrogen from ammonium is considered instead of atmospheric nitrogen. *A. ferrooxidans* requires oxygen as electron acceptor when it oxidizes Fe^{2+} to Fe^{3+}.

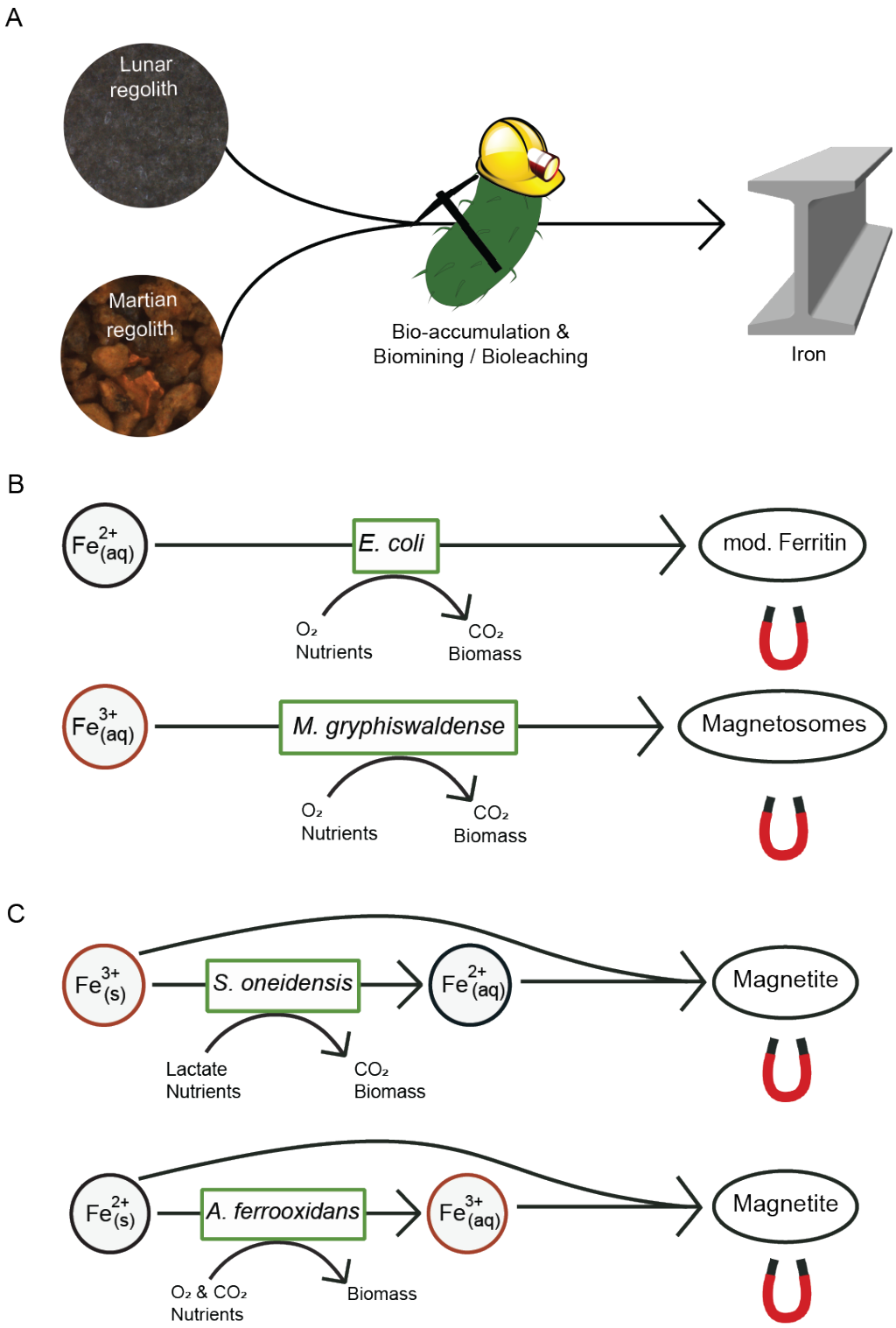

Figure 1. Workflow of the bacterial iron extraction. (A) The concept of using bacterial mining processes for the extraction of elemental iron, which can be used for material production. (B) Bio-accumulation processes using E. coli to bind aquatic Fe^{2+} in a modified Ferritin molecule, and M. gryphiswaldense to combine aquatic Fe^{3+} molecules in magnetosomes. (C) Biomining and Bioleaching approaches using S.oneidensis, to reduce in ore bound Fe^{3+} to Fe^{2+} and allow for magnetite precipitation, and A. ferroxidans to oxidize Fe^{2+} to Fe^{3+} and allow for magnetite precipitation.

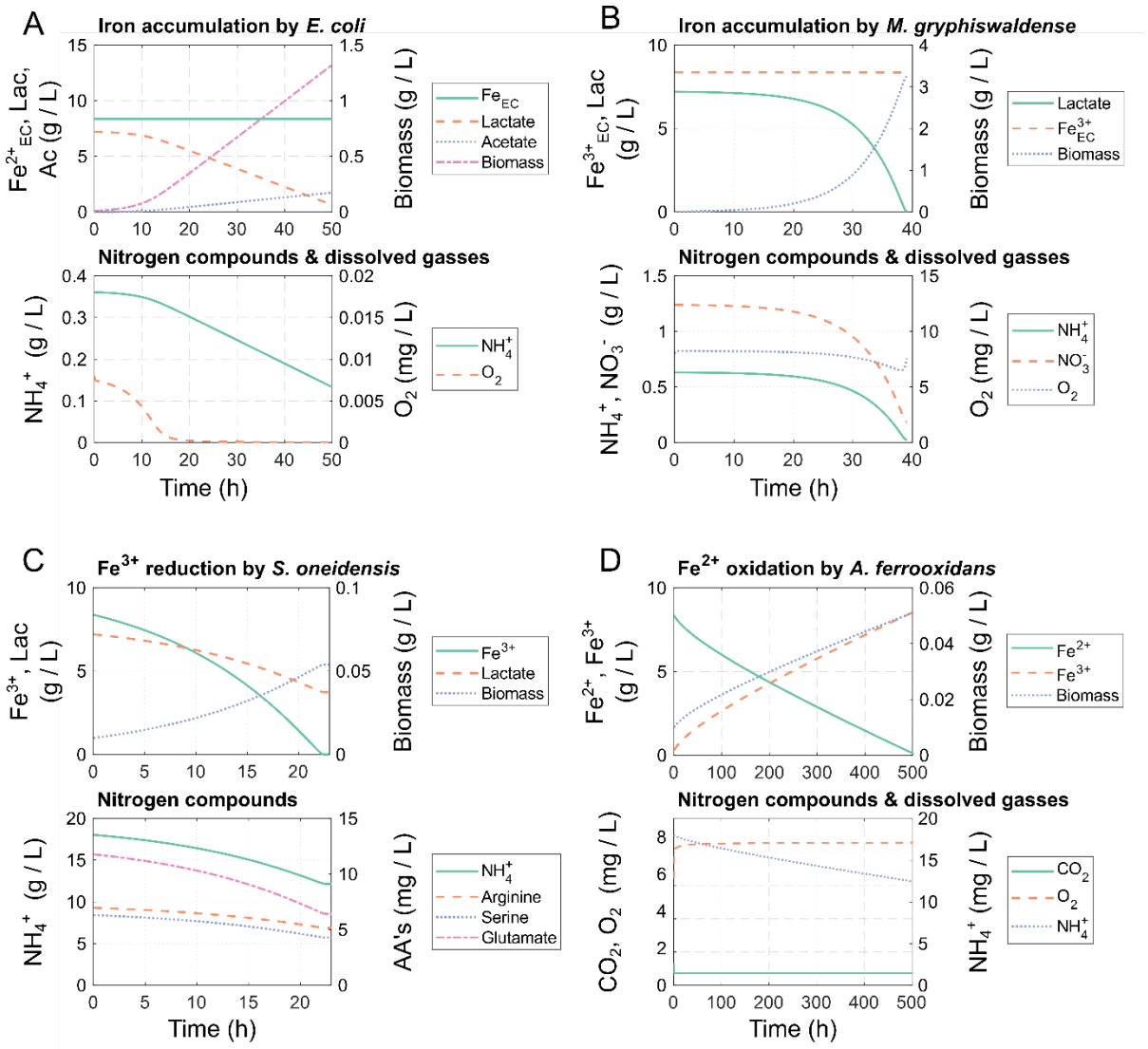

Figure 2. Literature-based growth models for *E. coli*, *M. gryphiswaldense*, *S. oneidensis* and *A. ferrooxidans*, showing nutrient consumption, dissolved gasses and iron dynamics. (A) Predicted growth and iron accumulation by *E. coli* with an overexpressed ferritin complex. After 10 hours, the oxygen transfer rate is predicted to be the limiting factor. The uptake of extracellular iron is negligible. (B) Predicted growth and iron accumulation by *M. gryphiswaldense*. The exponential growth rate is maintained until lactate is depleted. The uptake of extracellular iron is negligible. (C) Predicted growth and iron conversion for *S. oneidensis* reducing Fe^{3+} to Fe^{2+} from solid mineral substrates. Exponential growth is maintained until iron is depleted. AA's: Amino Acids (D) The predicted growth and iron conversion for *A. ferrooxidans* oxidizing Fe^{2+} to Fe^{3+}. Product inhibition by Fe^{3+} results in a linear growth profile.

3.1. Nutrient consumption

The kinetics (Table 1) were used to set up mass balances, which were solved over time to the point where one of the nutrients was used up (Fig 2). For an ideal process, the growth is expected to resemble batch growth, with an exponential increase in biomass concentration. In the accumulation processes by *E. coli* and *M. gryphiswaldense*, significant uptake of extracellular dissolved iron is expected. For the leaching processes by

S. oneidensis and *A. ferrooxidans*, the iron conversion is a key part of the organism's metabolism, so growth should be accompanied by a rapid iron conversion.

The accumulation process in *E. coli* (Fig 2A), takes slightly over 50 hours to consume the initially provided lactate (7.2 g/L). The predicted growth profile is initially exponential, but changes into a linear profile after 15 hours. The decreasing dissolved oxygen concentration indicates that the growth is limited by the oxygen transfer rate. If the process would show otherwise favorable results, methods for an increased oxygen transfer rate could be explored to decrease process time. However, the extracellular iron concentration does not decrease notably over the course of the simulation and thus the process does not fulfill its main purpose of accumulating dissolved iron. The overexpression of the encapsulated ferritin leads to an estimated 20-50 encapsulated ferritin complexes per cell, which corresponds to an iron concentration in biomass of only 8-20 µg / g_X. This value is too low to have a significant effect on the extracellular concentration.

The model for *M. gryphiswaldense* (Fig 2B) predicts batch growth for the full process and takes 39 hours to fully consume the initial lactate and ammonium. The decreasing level of dissolved oxygen indicates its consumption, but the oxygen transfer rate is not the limiting factor. Again, the concentration of extracellular iron does not decrease notably. *M. gryphiswaldense* reportedly accumulates iron to a concentration of 4.4 mg / g_X (Naresh et al., 2012), three orders of magnitude more than the proposed *E. coli* strain. Still, this is not enough to have a substantial impact on the extracellular iron concentration.

For the bio-accumulation of iron to be a feasible approach to ISRU activities, the amount of iron accumulated in one gram of biomass should outweigh the amount of transported nutrients required to generate that one gram of biomass. In the case of *M. gryphiswaldense* growing on lactate, that means that one gram of lean biomass should contain 2.8 grams of iron (Table 2), i.e. 74% of total biomass should be iron. For *E. coli* growing on lactate, these values are 7.73 gram and 88.5%. This requirement will become more lenient when the process is integrated with other biological systems. These systems can provide nutrients for the mining operation or make use of the byproducts of the process.

The process for Fe^{3+} reduction by *S. oneidensis* (Fig 2C) takes 22 hours to reduce all the initial Fe^{3+} and doesn't follow a full exponential growth curve. The growth rate slowly decreases from 80 to 70% of the μ_{max} value in the first 20 hours, and rapidly drops further after that. The reduction of the growth rate occurs due to a decrease of both the lactate and iron concentration. The acetate concentration (not shown) will increase over

the course of the process, mirroring the concentration profile of lactate. Acetate has an inhibitory effect on *S. oneidensis* (Tang et al., 2007), but the extent of that effect in anaerobic conditions has not been quantified.

The Fe^{2+} oxidation by *A. ferrooxidans* (Fig 2D) is by far the slowest process in the analysis and requires 500 hours to fully consume the initial iron. The slow process is mainly due to the inhibitory effect of Fe^{3+}. In the current model, no further reactions consuming dissolved Fe^{3+} or precipitation are considered, and the resulting continuous accumulation is detrimental for the growth rate of *A. ferrooxidans*. The dissolved gasses in the bottom panel show that no O_2 or CO_2 limitation is expected with the current growth rates.

Table 3. Mass-wise yields for the considered components in each process, normalized for the production of 1 gram biomass. All values in gram / gram biomass. Iron uptake in both *E. coli* and *M. gryphiswaldense* is multiple orders of magnitude smaller than the consumption of other nutrients.

	E. coli	***M. gryphiswaldense***	***S. oneidensis****	***A. ferrooxidans****
Fe^{2+}	$-2.1*10^{-5}$			
Fe^{3+}		$-4.4*10^{-3}$		200.7
Fe_2O_3 (Fe)			-817.74 (566)**	
FeO				-258.22
Fe_3O_4 (Fe)			790.45 (566)**	
Lactate	-4.95	-2.22	-78.90	
Acetate	1.31		51.64	
NH_4^+	-0.24	-0.19	-0.13	-0.13
NO_3^-		-0.33		
CO_2	3.62	0.65	37.84	-1.65
O_2	-2.61	-0.05		-27.60
H_2O	1.83		15.85	96.64
Arginine			$-41.1*10^{-3}$	
Serine			$-45.9*10^{-3}$	
Glutamate			-0.12	
HCl			-0.006	-392.9

*The *S. oneidensis* process considers the biological conversion of Fe^{3+} and precipitation of magnetite (Fe_3O_4) simultaneously, since both these processes occur at a similar pH-level. The *A. ferrooxidans* process considers just the biological conversion due to the low pH required for *A. ferrooxidans* growth.

** Equivalent Fe mass.

194 The yields and nutrient requirements of the four organisms were analyzed in further detail (Table 2). The
195 large difference between iron uptake and consumption of nutrients for both *E. coli* and *M. gryphiswaldense* is
196 emphasized once more. In the case of *S. oneidensis*, its essential amino acids were added to the equation to
197 evaluate their impact on the mass yield. Even though the amino acids are essential for growth, their impact in
198 terms of mass is negligible. In the *S. oneidensis* process, performed at a pH level of 7, the reduction of iron is
199 combined with the precipitation of magnetite. In this combination, the precipitation of magnetite is assumed to
200 be non-limiting and it is assumed to consume all bio-reduced iron. Since the biological process consumes
201 protons, but the precipitation produces protons, the combination results in only a very small acid consumption.
202 In the *A. ferrooxidans* process, performed at a pH level of 2, this combination is not possible, and thus a
203 large amount of acid is required to maintain the process pH. The resulting acid requirement, converted to a mass
204 of HCl, is larger than the amount of leached iron, which makes this process unfeasible.
205 There are several key changes for bioprocesses carried out on the moon or mars as opposed to those carried
206 out on earth. Radiation doses on the Moon and Mars are significantly higher than those on earth. However,
207 comparison of the yearly Martian surface dose of 0.242 Sv (Simonsen et al., 1990) with the minimal effects of
208 an acute radiation dose of 12 Sv on the growth profile and biomass yield of *S. oneidensis* (Brown et al., 2015)
209 leads to the conclusion that radiation effects are likely negligible (Volger et al. manuscript submitted).
210 Furthermore, the process will be carried out under lower gravity, which will impact fluid dynamics, but might
211 also have an impact on bacterial performance (Demey et al., 2000; Kacena et al., 1999). On top of that, the
212 composition of the local regolith can have a negative effect on survival rates of some organisms, such as the
213 case with perchlorates in the Martian soil.

214 *3.2. Bacterial survivability on Martian regolith*

215 The bacterial survivability if they are mixed with Martian regolith is a key factor for the successful
216 appliance of bacterial *in situ* resource utilization (bISRU). *S. oneidensis* was, therefore, added and grown in two
217 different concentrations of JSC-Mars1 intermixed with magnesium perchlorate, which was reported of being
218 toxic to a variety of organisms (Al Soudi et al., 2017; Wadsworth and Cockell, 2017) and abundant on the
219 Martian surface. First, the bacteria were observed via 3D microscopy while growing in a high concentration
220 setting with about 50 g/L JSC1-MARS1 (Fig 3AB). To quantify the so-obtained data and test the effect of the
221 perchlorates optical density (OD) measurements at a wavelength of 600 nm were performed. The concentration
222 of the iron (and so the entire regolith simulant) had to be lowered to 0.5 g/L and 5 g/L for the planktonic culture

to limit the effect of light reflection by the ore-particles at this wavelength. The growth curves of two different sub strains of *S. oneidensis* (MR1 and ANA 3) showed no differences between the tryptic soy broth (TSB) control, the 0.5 g/L JSC-MARS1 control and the 0.5 g/L JSC-MARS1 mixed with 0.05 M magnesium perchlorate (Fig. 3C). The no-bacteria control of the JSC-MARS1 medium together with the 0.05 M magnesium perchlorate showed a strong fluctuation. This might be due to the acidity of perchloric acid and its interaction and oxidation of the regolith ores in the aquatic solution (Jackson et al., 2006). The increased baseline and fluctuations of the OD_{650} curves was even more severe in the samples with 5 g/L JSC-MARS1 (Fig. 3D). The ΔOD_{650} and, therefore, the growth of the bacteria seems to be lower in the JSC-Mars1 and JSC-MARS1+$Mg(ClO_4)_2$ samples, but these results are not significant because of the high fluctuations. With the lower concentration of regolith simulant and perchlorate *S. oneidensis* MR1 and ANA3 growth is not influenced for high concentrations of regolith a quantification is barely possible but the visual check of 3D microscopy showed normal growth activity.

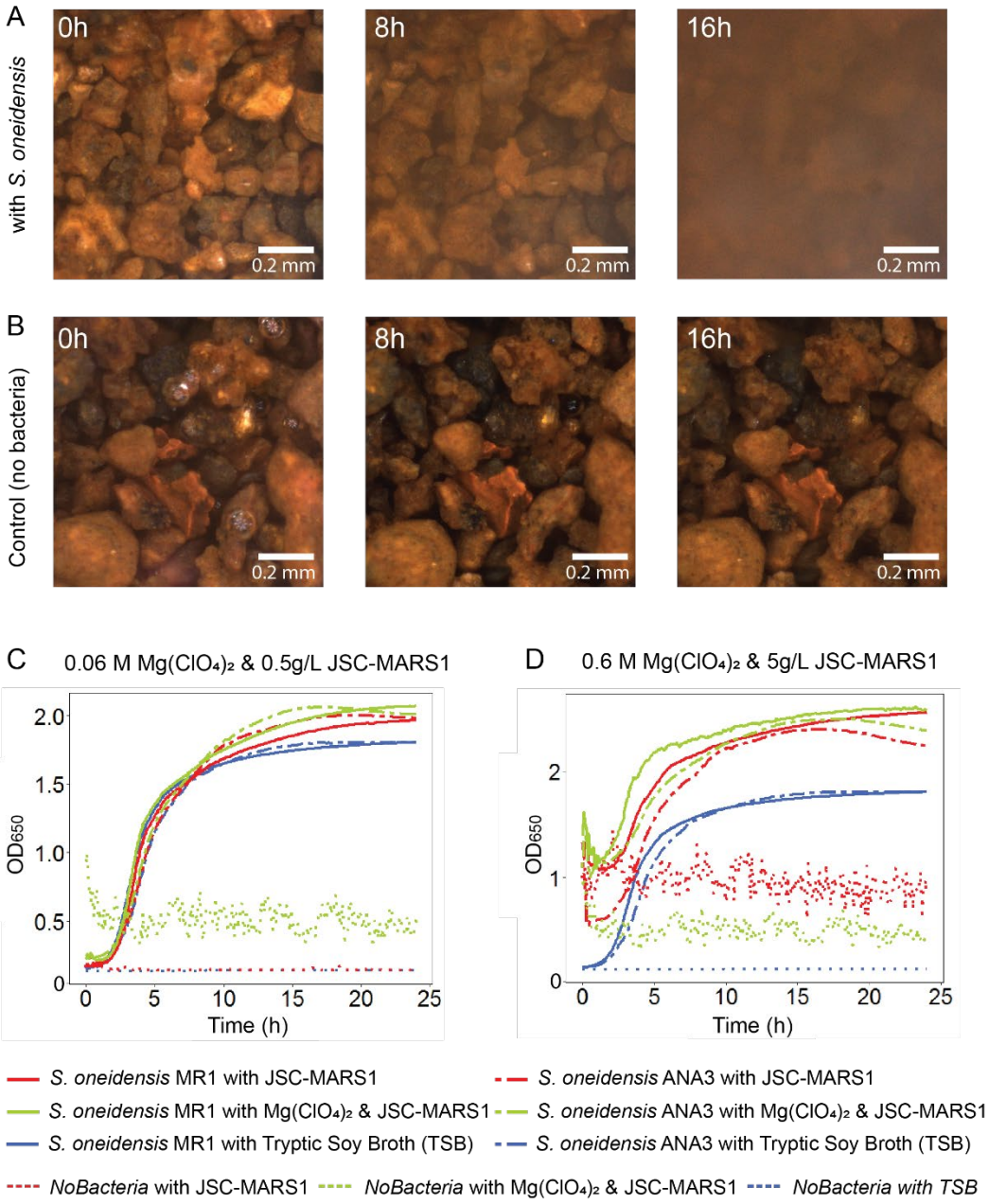

Figure 3. Growth of *S. oneidensis* MR1 and ANA3 in Martian regolith simulant (JSC-MARS1). (A) Bacterial growth observed via a 3D microscopy approach. After 8 hours we see a increase in the bacterial sample and after 16 hours the regolith particles are barely visible any more. (B) Control experiment without bacteria. No change in the 3D microscopy pictures was observed. (C) Bacterial growth of *S. oneidensis* ANA3 & MR1 under the influence of 0.5 g/L Mars regolith simulant (JSC-MARS1) and 0.06 mol/L magnesium perchlorate. No differences in the growth behavior was seen. (D) Bacterial growth of *S. oneidensis* ANA3 & MR1 under the influence of 5 g/L Mars regolith simulant (JSC-MARS1) and 0.6 mol/L magnesium perchlorate. The baseline of the control was shifted due to the higher number of particles in the solution. The absolute growth rate was not influenced.

3.3. Payback time analysis

The *S. oneidensis* process was used for a further analysis, where the process performance was combined with estimated bioreactor lander characteristics (Volger et al., 2018) to calculate the payback time of the entire

process (Figure 4). This process uses ferric iron (Fe^{3+}) as a starting material, and thus is focused on Martian applications. The process consists of three distinct phases:

1. Intake phase: Fresh regolith is loaded in the reactor, water and nutrients are added and finally inoculated with a small amount of *S. oneidensis* biomass.
2. Growth phase: *S. oneidensis* grows exponentially and leaches iron from the regolith.
3. Extraction phase. Magnetite and other magnetically active minerals are separated from the rest of the medium, the water is evaporated and recycled, and the rest of the regolith is sterilized and disposed.

The duration of the growth phase is determined with the kinetics from table 1, while the other two phases combined are assumed to take 24 hours. The minimal payback time is defined as the moment where the mass of extracted iron exceeds the initial mass of the lander.

The impact of several parameters on the payback time was investigated (Fig 4). An increase in initial biomass concentration will lead to a faster process and increased mass gains per hour, but more inoculate from a frozen stock (assumed 10 g_X / L) is needed per run, increasing the required transported mass (Fig 4A). These effects counteract each other; when the initial biomass is increased up to 5 mg / L, the payback time decreases, but any further increase result in a decrease of the overall performance. The optimal initial biomass concentration for the base case was found to be 4.5 mg / L.

The efficiency of the water recycling step was varied, and it was found that a certain minimal efficiency was required (Fig 4B). At lower efficiencies, the process loses more water than it gains in iron. Higher efficiency always leads to a better payback time. For the base case, with an initial iron concentration of 0.27 mol / L, the minimum required recycling efficiency is 99.79%. For most further analyses, a water recycling efficiency of 99.9% is assumed (Fu et al., 2016), unless stated otherwise.

If the process starts with a higher iron concentration, a higher amount of iron is extracted at the end of the process, which weighs up against the water loss in the recycling steps. On top of that, a higher initial iron concentration increases the duration of the growth phase, so the productive time per run increases. With the water recycling efficiency of 99.79% (Fig. 4C left), the base case initial iron concentration of 0.27 mol / L was also found to be the minimum required for a positive payback time. If the water recycling efficiency was increased to 99.90% (Fig. 4C right), the minimum initial iron concentration decreased to 0.13 mol / L. The further rise to infinity when approaching this value and asymptote were cut off the figure due to the axis bounds. Higher initial iron concentrations always lead to a reduced payback time. It should be noted that mixing issues

due to the resulting slurry and abrasion issues from the increased regolith concentration have not been considered and so no maximum concentration will be found with the current models.

The relation between minimum water recycling efficiency and minimum initial iron concentration was further investigated, and a linear relation between the two was found (Fig 4D). The higher the water recycling efficiency, the lower the initial iron concentration needs to be to find a positive payback time. A combination of very efficient water recycling and high initial iron concentration leads to lower payback times.

The environment of another celestial body can have an impact on the performance of a bioprocess. The increased radiation and altered gravity can lead to increased stress for the organism, changing its performance. This effect was simulated by changing the maximal growth rate and analyzing the effect on the payback time (Fig 4E). The process was found to be sensitive to low growth rates, with high sensitivity between 0 and 0.3 h^{-1}. The chosen growth rate of 0.1 h^{-1} is in this regime, so a small change in the growth rate will have a large impact on the payback time. The insights about the different parameters were combined, and a payback time of 3.3 years was found at a water recycling efficiency of 99.99%, an initial iron concentration of 0.8 mol / L (300 g regolith / L) and an initial biomass concentration of 0.088 g / L. Addition of Martian ice water can reduce the required water recycling efficiency to more achievable levels.

Independent of the exact biological properties, the fact that bioprocesses take place in watery solutions results in general process limitations. A key tradeoff is that high concentrations of solids will lead to impaired mixing and reduced gas-liquid mass transfer, but at the same time these high solids concentrations result in more concentrated iron output. Assuming a maximum regolith concentration of 500 g / L with an iron content of ~15%, a maximum of 75 g iron will be extracted with one liter of biological culture. This puts a lower limit on the water recycling efficiency: a 92.5% recycling efficiency is required to extract more iron than the lost water. When ores with higher iron concentration are fed, lower water recycling efficiency is required; at 22% iron the minimum water recycling efficiency is 88.9%. Dependent on the characteristics of mixing in reduced gravity and iron content of the ores, a precise maximum solids concentration and minimum recycling efficiency can be determined.

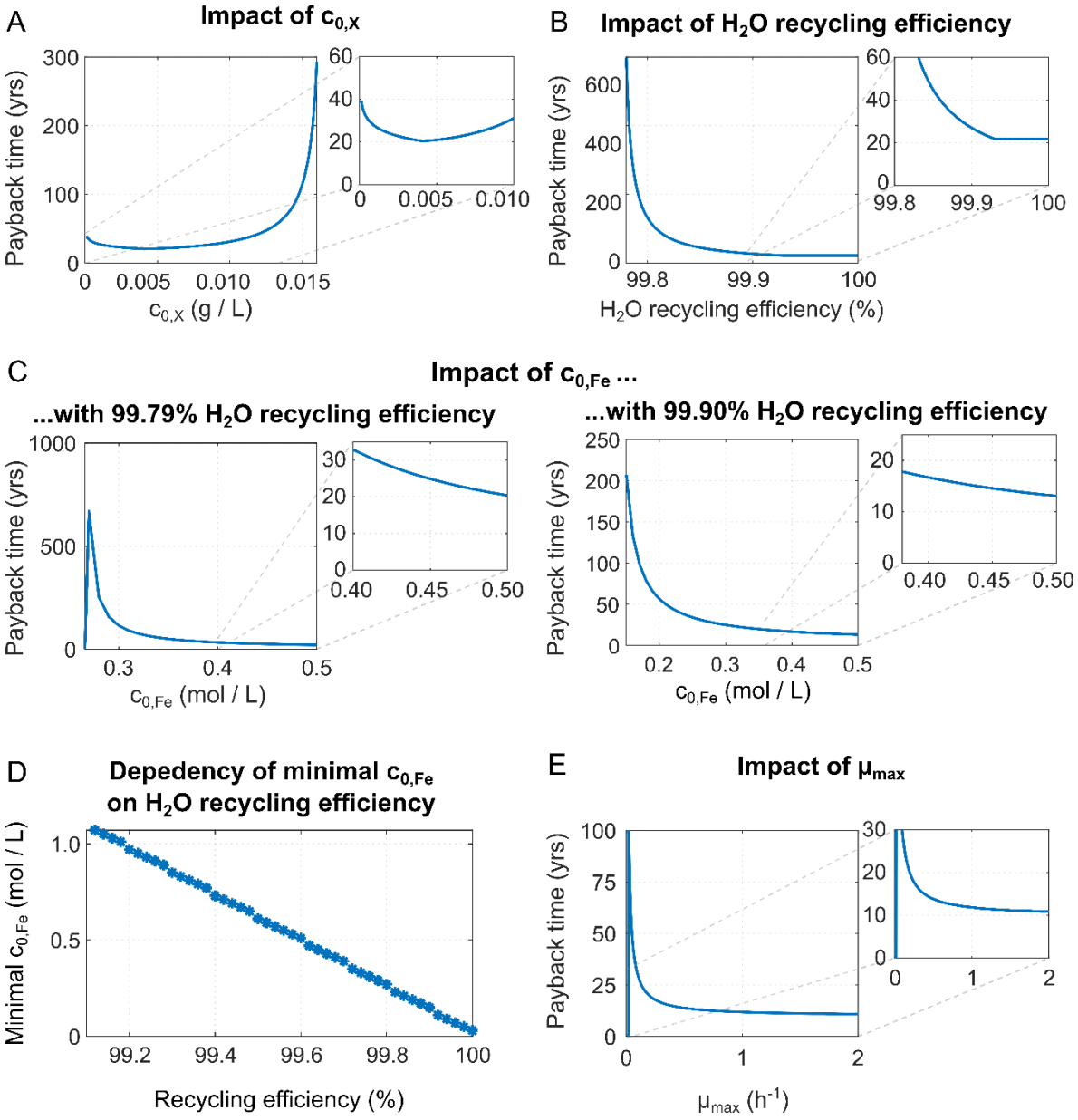

Figure 4. Sensitivity analysis on the mass-dependent payback time. (A) Impact of initial biomass concentration on process payback time, assuming 99.9% water recycling efficiency. Asymptotic behavior is observed when the initial biomass concentration exceeds 0.014 g / L. (B) Payback time shows high sensitivity to the water recycling efficiency. A higher water recycling efficiency leads to lower payback times. Asymptotic behavior is observed when recycling efficiency drops below 99.8%. (C) Impact of initial iron concentration both with 99.79% water recycling efficiency and 99.90% recycling efficiency. The payback time decreases with increasing initial iron concentration and the asymptote shifts with changes in water recycling efficiency. (D) The linear relation between water recycling efficiency and minimum required initial iron concentration for a positive payback time is displayed. (E) The impact of maximum growth rate (μ_{max}) on payback time, assuming 99.9% water recycling efficiency, is shown. A higher μ_{max} leads to shorter payback times and asymptotic behavior is observed when μ_{max} drops below 0.02 h^{-1}. The payback time shows high sensitivity in the range 0-0.3 h^{-1}.

4. Conclusion

In this paper, a general process setup for biological extraction of iron from Lunar or Martian regolith is presented, consisting of a leaching step and an accumulation or precipitation step. These are combined with a magnetic extraction to obtain the iron-rich minerals. Four organisms were investigated for their use in either an

iron leaching or iron accumulation step. Their yields and kinetics were derived from elemental balancing and literature, and kinetic models were set up. *M. gryphiswaldense*, modified *E. coli* and *A. ferrooxidans* were found to be incompatible with the envisioned process due to a disappointing level of accumulation and low yield. Their nutrient requirements outweigh the extracted iron, which makes the process inherently infeasible with transported nutrients. In the case of *A. ferrooxidans*, the most important factor was the acid consumption, something that needs close attention in the analysis of bioprocesses. If the acids could be provided *in-situ A. ferrooxidans* would be an optimal organism for bioleaching on the iron(II) rich Moon.

S. oneidensis was identified as a promising candidate, with an iron yield of 2.5 g / $g_{nutrients}$ for just the biological conversion, and a yield of 7.14 g / $g_{nutrients}$ after combination with magnetite precipitation. This combination also minimizes the acid consumption of the process. The effect of JSC-Mars1 and $Mg(ClO_4)_2$ on the growth of *S. oneidensis* was found to be small, a promising feature for application for Martian exploration.

The payback time of the process utilizing *S. oneidensis* was analyzed, and the sensitivity to various parameters was investigated. Key factors for a feasible process are highly efficient water recycling and a high initial concentration of iron. With a water recycling efficiency of 99.99% and initial iron concentration of 0.8 mol / L, a payback time of less than 4 years can be achieved. The current conclusions are based on literature data and will rely on further experimental work with *S. oneidensis*.

The process setup assumes a watery or slurry-like solution. Other modes of operation, such as a trickle bed reactor, could provide higher or longer productivity in the same volume of water due to a higher amount of solids per volume of liquid and continuous waste removal. Lower water requirements can counteract the negative effects of water losses and thus increase the potential of biological ISRU processes.

5. Acknowledgement

Our thanks to the Spaceship EAC team in Cologne for interesting discussions and input. This work was supported by the Netherlands Organization for Scientific Research (NWO/OCW), as part of the Frontiers of Nanoscience program.

6. References

Al Soudi, A.F., Farhat, O., Chen, F., Clark, B.C., Schneegurt, M.A., 2017. Bacterial growth tolerance to concentrations of chlorate and perchlorate salts relevant to Mars. Int. J. Astrobiol. 16, 229–235. https://doi.org/10.1017/S1473550416000434

Bale, C.W., Bélisle, E., Chartrand, P., Decterov, S.A., Eriksson, G., Gheribi, A.E., Hack, K., Jung, I.-H., Kang, Y.-B., Melançon, J., Pelton, A.D., Petersen, S., Robelin, C., Sangster, J., Spencer, P., Van Ende, M.-A., 2016. FactSage thermochemical software and databases, 2010–2016. https://doi.org/10.1016/j.calphad.2016.05.002

328 Bennett, B.D., Brutinel, E.D., Gralnick, J.A., 2015. A Ferrous Iron Exporter Mediates Iron Resistance in
329 Shewanella oneidensis MR-1. Appl. Environ. Microbiol. 81, 7938–7944.
330 https://doi.org/10.1128/AEM.02835-15

331 Brown, A.R., Correa, E., Xu, Y., AlMasoud, N., Pimblott, S.M., Goodacre, R., Lloyd, J.R., 2015. Phenotypic
332 Characterisation of Shewanella oneidensis MR-1 Exposed to X-Radiation. PLoS One 10, e0131249.
333 https://doi.org/10.1371/journal.pone.0131249

334 Carpenter, J., Fisackerly, R., Houdou, B., 2016. Establishing lunar resource viability. Space Policy 37, 52–57.
335 https://doi.org/10.1016/J.SPACEPOL.2016.07.002

336 Cousins, C.R., Cockell, C.S., 2016. An ESA roadmap for geobiology in space exploration. Acta Astronaut. 118,
337 286–295. https://doi.org/10.1016/j.actaastro.2015.10.022

338 Culbert, C., Linne, D., Chandler, F., Alexander, L., Jefferies, S., Kennedy, K.J., Lupisella, M., Metzger, P.,
339 Moore, N., Taminger, K., 2015. NASA Technology Roadmaps - TA 7: Human Exploration Destination
340 Systems.

341 Demey, D., Hermans, V., Cornet, J.-F., Leclercq, J.-J., Lasseur, C., Delahaye, A., 2000. BIORAT: Preliminary
342 Evaluation of Biological Life Support in Space Environment. https://doi.org/10.4271/2000-01-2384

343 Doran, P.M., 2013. Bioprocess engineering principles, 2nd ed. Elsevier/Academic Press.

344 Dumbacher, D., 2014. “Fact checking rumors on NASA’s Space Launch System” by Jason Rhian [WWW
345 Document]. URL https://www.spaceflightinsider.com/organizations/nasa/fact-check-sls-rumors/
346 (accessed 10.20.19).

347 Feng, X., Xu, Y., Chen, Y., Tang, Y.J., 2012. Integrating Flux Balance Analysis into Kinetic Models to
348 Decipher the Dynamic Metabolism of Shewanella oneidensis MR-1. PLoS Comput. Biol. 8, e1002376.
349 https://doi.org/10.1371/journal.pcbi.1002376

350 Fu, Y., Li, L., Xie, B., Dong, C., Wang, M., Jia, B., Shao, L., Dong, Y., Deng, S., Liu, Hui, Liu, G., Liu, B.,
351 Hu, D., Liu, Hong, 2016. How to Establish a Bioregenerative Life Support System for Long-Term Crewed
352 Missions to the Moon or Mars. Astrobiology 16, 925–936. https://doi.org/10.1089/ast.2016.1477

353 Halliday, A.N., Wänke, H., Birck, J.-L., Clayton, R.N., 2001. The Accretion, Composition and Early
354 Differentiation of Mars. Space Sci. Rev. 96, 197–230. https://doi.org/10.1023/A:1011997206080

355 He, D., Hughes, S., Vanden-Hehir, S., Georgiev, A., Altenbach, K., Tarrant, E., Mackay, C.L., Waldron, K.J.,
356 Clarke, D.J., Marles-Wright, J., 2016. Structural characterization of encapsulated ferritin provides insight
357 into iron storage in bacterial nanocompartments. Elife 5. https://doi.org/10.7554/eLife.18972

358 Hua, Q., Joyce, A.R., Palsson, B.O., Fong, S.S., 2007. Metabolic Characterization of Escherichia coli Strains
359 Adapted to Growth on Lactate. Appl. Environ. Microbiol. 73, 4639–4647.
360 https://doi.org/10.1128/AEM.00527-07

361 Jackson, W.A., Anderson, T., Harvey, G., Orris, G., Rajagopalan, S., Kang, N., 2006. Occurrence and
362 Formation of Non-Anthropogenic Perchlorate, in: Perchlorate: Environmental Occurrence, Interactions
363 and Treatment. Kluwer Academic Publishers, Boston, pp. 49–69. https://doi.org/10.1007/0-387-31113-
364 0_3

365 Kacena, M.A., Merrell, G.A., Manfredi, B., Smith, E.E., Klaus, D.M., Todd, P., 1999. Bacterial growth in space
366 flight: logistic growth curve parameters for Escherichia coli and Bacillus subtilis. Appl. Microbiol.
367 Biotechnol. 51, 229–234. https://doi.org/10.1007/s002530051386

368 Kane, A.L., Brutinel, E.D., Joo, H., Maysonet Sanchez, R., VanDrisse, C.M., Kotloski, N.J., Gralnick, J.A.,
369 2016. Formate Metabolism in *Shewanella oneidensis* Generates Proton Motive Force and Prevents
370 Growth Without an Electron Acceptor. J. Bacteriol. 198, JB.00927-15. https://doi.org/10.1128/JB.00927-
371 15

372 Kostka, J.E., Dalton, D.D., Skelton, H., Dollhopf, S., Stucki, J.W., 2002. Growth of Iron(III)-Reducing Bacteria
373 on Clay Minerals as the Sole Electron Acceptor and Comparison of Growth Yields on a Variety of
374 Oxidized Iron Forms. Appl. Environ. Microbiol. 68, 6256–6262.

https://doi.org/10.1128/AEM.68.12.6256-6262.2002

Kostka, J.E., Stucki, J.W., Nealson, K.H., Wu, J., 1996. Reduction of Structural Fe(III) in Smectite by a Pure Culture of Shewanella Putrefaciens Strain MR-1. Clays Clay Miner. 44, 522–529. https://doi.org/10.1346/CCMN.1996.0440411

Lawrence, D.J., Feldman, W.C., Elphic, R.C., Little, R.C., Prettyman, T.H., Maurice, S., Lucey, P.G., Binder, A.B., 2002. Iron abundances on the lunar surface as measured by the Lunar Prospector gamma-ray and neutron spectrometers. J. Geophys. Res. Planets 107, 13-1-13–26. https://doi.org/10.1029/2001JE001530

Lefèvre, C.T., Abreu, F., Lins, U., Bazylinski, D.A., 2011. A Bacterial Backbone: Magnetosomes in Magnetotactic Bacteria, in: Metal Nanoparticles in Microbiology. Springer Berlin Heidelberg, Berlin, Heidelberg, pp. 75–102. https://doi.org/10.1007/978-3-642-18312-6_4

Lehner, B.A.E., Schlechten, J., Filosa, A., Canals Pou, A., Mazzotta, D.G., Spina, F., Teeney, L., Snyder, J., Tjon, S.Y., Meyer, A.S., Brouns, S.J.J., Cowley, A., Rothschild, L.J., 2019. End-to-end mission design for microbial ISRU activities as preparation for a moon village. Acta Astronaut. 162, 216–226. https://doi.org/10.1016/J.ACTAASTRO.2019.06.001

Liu, C., Gorby, Y.A., Zachara, J.M., Fredrickson, J.K., Brown, C.F., 2002. Reduction kinetics of Fe(III), Co(III), U(VI), Cr(VI), and Tc(VII) in cultures of dissimilatory metal-reducing bacteria. Biotechnol. Bioeng. 80, 637–649. https://doi.org/10.1002/bit.10430

Liu, M.S., Branion, R.M.R., Duncan, D.W., 1988. The effects of ferrous iron, dissolved oxygen, and inert solids concentrations on the growth of thiobacillus ferrooxidans. Can. J. Chem. Eng. 66, 445–451. https://doi.org/10.1002/cjce.5450660315

Lovley, D.R., Phillips, E.J.P., Lonergan, D.J., 1989. Hydrogen and Formate Oxidation Coupled to Dissimilatory Reduction of Iron or Manganese by Alteromonas putrefaciens. Appl. Environ. Microbiol. 55, 700–706.

Lozano, I., Casillas, N., de León, C.P., Walsh, F.C., Herrasti, P., 2017. New Insights into the Electrochemical Formation of Magnetite Nanoparticles. J. Electrochem. Soc. 164, D184–D191. https://doi.org/10.1149/2.1091704jes

Molchanov, S., Gendel, Y., Ioslvich, I., Lahav, O., 2007. Improved experimental and computational methodology for determining the kinetic equation and the extant kinetic constants of Fe(II) oxidation by Acidithiobacillus ferrooxidans. Appl. Environ. Microbiol. 73, 1742–52. https://doi.org/10.1128/AEM.01521-06

Myers, C.R., Nealson, K.H., 1988. Bacterial Manganese Reduction and Growth with Manganese Oxide as the Sole Electron Acceptor. Science (80-.). 240, 1319–1321. https://doi.org/10.1126/science.240.4857.1319

Naresh, M., Das, S., Mishra, P., Mittal, A., 2012. The chemical formula of a magnetotactic bacterium. Biotechnol. Bioeng. 109, 1205–1216. https://doi.org/10.1002/bit.24403

NASA, 2018. The Global Exploration Roadmap 2018.

Navarrete, J.U., Cappelle, I.J., Schnittker, K., Borrok, D.M., 2013. Bioleaching of ilmenite and basalt in the presence of iron-oxidizing and iron-scavenging bacteria. Int. J. Astrobiol. 12, 123–134. https://doi.org/10.1017/S1473550412000493

Neale, J.W., Pinches, A., 1994. Determination of gas-liquid mass-transfer and solids-suspension parameters in mechanically-agitated three-phase slurry reactors. Miner. Eng. 7, 389–403. https://doi.org/10.1016/0892-6875(94)90078-7

Núñez, M.F., Kwon, O., Wilson, T.H., Aguilar, J., Baldoma, L., Lin, E.C.C., 2002. Transport of L-Lactate, D-Lactate, and Glycolate by the LldP and GlcA Membrane Carriers of Escherichia coli. https://doi.org/10.1006/bbrc.2001.6255

Perez-Gonzalez, T., Jimenez-Lopez, C., Neal, A.L., Rull-Perez, F., Rodriguez-Navarro, A., Fernandez-Vivas, A., Iañez-Pareja, E., 2010. Magnetite biomineralization induced by Shewanella oneidensis. Geochim. Cosmochim. Acta 74, 967–979. https://doi.org/10.1016/j.gca.2009.10.035

Pettit, D.R., Allen, D.T., 1992. Unit Operations for Gas-Liquid Mass Transfer in Reduced Gravity

Environments, in: The Second Conference on Lunar Bases and Space Activities of the 21st Century, Volume 2. NASA. Johnson Space Center, p. p 647-651.

Pinchuk, G.E., Hill, E.A., Geydebrekht, O. V., De Ingeniis, J., Zhang, X., Osterman, A., Scott, J.H., Reed, S.B., Romine, M.F., Konopka, A.E., Beliaev, A.S., Fredrickson, J.K., Reed, J.L., 2010. Constraint-Based Model of Shewanella oneidensis MR-1 Metabolism: A Tool for Data Analysis and Hypothesis Generation. PLoS Comput. Biol. 6, e1000822. https://doi.org/10.1371/journal.pcbi.1000822

Potter, R., Saikia, S., Longuski, J., 2018. Resilient architecture pathways to establish and operate a pioneering base on Mars, in: IEEE Aerospace Conference Proceedings. IEEE Computer Society, pp. 1–18. https://doi.org/10.1109/AERO.2018.8396506

R. Dasgupta, D., L. Mackay, A., 1959. β-Ferric Oxyhydroxide and Green Rust. J. Phys. Soc. Japan 14, 932–935. https://doi.org/10.1143/JPSJ.14.932

Rawlings, D.E., 2002. Heavy Metal Mining Using Microbes. Annu. Rev. Microbiol 56, 65–91. https://doi.org/10.1146/annurev.micro.56.012302.161052

Schippers, A., Hedrich, S., Vasters, J., Drobe, M., Sand, W., Willscher, S., 2013. Biomining: Metal Recovery from Ores with Microorganisms. Springer, Berlin, Heidelberg, pp. 1–47. https://doi.org/10.1007/10_2013_216

Schüler, D., Baeuerlein, E., 1998. Dynamics of iron uptake and Fe3O4 biomineralization during aerobic and microaerobic growth of Magnetospirillum gryphiswaldense. J. Bacteriol. 180, 159–62.

Schumpe, A., Saxena, A.K., Fang, L.K., 1987. Gas/liquid mass transfer in a slurry bubble column. Chem. Eng. Sci. 42, 1787–1796. https://doi.org/10.1016/0009-2509(87)80183-5

Simonsen, L.C., Nealy, J.E., Townsend, L.W., Wilson, J.W., 1990. Space Radiation Shielding for a Martian Habitat. SAE Trans. 99, 972--979. https://doi.org/10.2307/44472557

SpaceX, 2019. Capabilities & Services | SpaceX [WWW Document]. URL https://www.spacex.com/about/capabilities (accessed 10.20.19).

Tang, Y.J., Meadows, A.L., Keasling, J.D., 2007. A kinetic model describing Shewanella oneidensis MR-1 growth, substrate consumption, and product secretion. Biotechnol. Bioeng. 96, 125–133. https://doi.org/10.1002/bit.21101

Valdés, J., Pedroso, I., Quatrini, R., Dodson, R.J., Tettelin, H., Blake, R., Eisen, J.A., Holmes, D.S., 2008. Acidithiobacillus ferrooxidans metabolism: from genome sequence to industrial applications. BMC Genomics 9, 597. https://doi.org/10.1186/1471-2164-9-597

Van Weert, G., Van Der Werff, D., Derksen, J.J., 1995. Transfer of O2 from air to mineral slurries in a rushton turbine agitated tank. Miner. Eng. 8, 1109–1124. https://doi.org/10.1016/0892-6875(95)00076-3

Volger, R., Brouns, S.J.J., Cowley, A., Picioreanu, C., Lehner, B.A.E., 2018. Bioreactor design to perform microbial mining activities on another celestial body, in: 69th International Astronautical Congress. Bremen.

Wadsworth, J., Cockell, C.S., 2017. Perchlorates on Mars enhance the bacteriocidal effects of UV light. Sci. Rep. 7, 4662. https://doi.org/10.1038/s41598-017-04910-3

Wang, G., Qian, F., Saltikov, C.W., Jiao, Y., Li, Y., 2011. Microbial reduction of graphene oxide by Shewanella. Nano Res. 4, 563–570. https://doi.org/10.1007/s12274-011-0112-2

Weber, K.A., Achenbach, L.A., Coates, J.D., 2006. Microorganisms pumping iron: Anaerobic microbial iron oxidation and reduction. Nat. Rev. Microbiol. 4, 752–764. https://doi.org/10.1038/nrmicro1490

Yin, S., Wang, L., Kabwe, E., Chen, X., Yan, R., An, K., Zhang, L., Wu, A., 2018. Copper Bioleaching in China: Review and Prospect. Minerals 8, 32. https://doi.org/10.3390/min8020032

Zokaei-Kadijani, S., Safdari, J., Mousavian, M.A., Rashidi, A., 2013. Study of oxygen mass transfer coefficient and oxygen uptake rate in a stirred tank reactor for uranium ore bioleaching. Ann. Nucl. Energy 53, 280–287. https://doi.org/10.1016/J.ANUCENE.2012.07.036